

Thermal H₂O emission from the Herbig-Haro flow HH 54*

R. Liseau^{1,2}, C. Ceccarelli^{3,2}, B. Larsson¹, B. Nisini², G.J. White⁴, P. Ade⁴, C. Armand⁵, M. Burgdorf⁵, E. Caux⁶, R. Cerulli², S. Church⁷, P.E. Clegg⁴, A. Di Gorgio^{5,2}, I. Furniss⁸, T. Giannini², W. Glencross⁸, C. Gry^{5,9}, K. King¹⁰, T. Lim⁵, D. Lorenzetti¹¹, S. Molinari^{5,2}, D. Naylor¹², R. Orfei², P. Saraceno², S. Sidher⁵, H. Smith⁴, L. Spinoglio², B. Swinyard¹⁰, D. Texier⁵, E. Tommasi², N. Trams⁵, and S. Unger¹⁰

¹ Stockholm Observatory, S-133 36 Saltsjöbaden, Sweden, (rene@astro.su.se)

² CNR-Istituto di Fisica dello Spazio Interplanetario, Casella Postale 27, I-00044 Frascati (Rome), Italy

³ Laboratoire d'Astrophysique de l'Observatoire de Grenoble, 414, rue de la Piscine, BP 53, F-38041 Grenoble, France

⁴ Physics Department, Queen Mary & Westfield College, University of London, Mile End Road, London E1 4NS, UK

⁵ The Lws Instrument-Dedicated Team, Iso Science Operations Centre, P.O. Box 50727, E-28080 Madrid, Spain

⁶ Centre d'Etude Spatiale des Rayonnements, BP 4346, F-31029 Toulouse Cedex, France

⁷ California Institute of Technology, Pasadena, CA 91125, USA

⁸ Department of Physics and Astronomy, University College London, Gower Street, London, WC1 E 6BT, UK

⁹ Laboratoire d'Astronomie Spatiale, BP8, F-13376 Marseille Cedex 12, France

¹⁰ Space Science Department, Rutherford Appleton Laboratory, Chilton, Oxon OX11 0QX, UK

¹¹ Osservatorio Astronomico di Roma, I-00044 Monteporzio, Italy

¹² Department of Physics, University of Lethbridge, Lethbridge, Alberta T1K 3M4, Canada

Received 2 July 1996 / Accepted 20 August 1996

Abstract. The first detection of thermal water emission from a Herbig-Haro object is presented. The observations were performed with the LWS (Long Wavelength Spectrograph) aboard ISO (Infrared Space Observatory). Besides H₂O, rotational lines of CO are present in the spectrum of HH 54. These high-*J* CO lines are used to derive the physical model parameters of the FIR (far-infrared) molecular line emitting regions. This model fits simultaneously the observed OH and H₂O spectra for an OH abundance $X(\text{OH}) = 10^{-6}$ and a water vapour abundance $X(\text{H}_2\text{O}) = 10^{-5}$.

At a distance of 250 pc, the total CO, OH and H₂O rotational line cooling rate is estimated to be $1.3 \cdot 10^{-2} L_{\odot}$, which is comparable to the mechanical luminosity generated by the 10 km s^{-1} shocks, suggesting that practically all of the cooling of the *weak-shock* regions is done by these three molecular species alone.

Key words: stars: formation – ISM: molecules – ISM: jets and outflows – ISM: individual objects: HH 54 – physical processes: shock waves – physical processes: radiative transfer

1. Introduction

The Herbig-Haro object HH 54 is associated with the star forming dark cloud Cha II, at a distance $d = 250$ pc, although this is uncertain by as much as $\gtrsim 100$ pc. The object consists of several arcsecond scale bright knots enveloped by diffuse emission ($\sim 40''$; Graham & Hartigan 1988). The overall optical emission line spectrum is indicative of the presence of relatively highly excited gas and can be explained with J-shocks of velocities of at least 60 km s^{-1} (Schwartz & Dopita 1980). Considerably lower velocities, of $\sim 10 \text{ km s}^{-1}$, are observed in the CO (1–0) emission from a cold (~ 15 K), extended molecular flow, whose emission peaks $\gtrsim 3'$ away from HH 54 (Knee 1992). Recent NIR (near-infrared) observations by Gredel (1994) testify to the presence of warm, purely collisionally excited, H₂ gas. This rather hot gas [~ 2000 K, $N(\text{H}_2) = 3.6 \cdot 10^{17} \text{ cm}^{-2}$] might be expected to emit strongly in relatively highly excited rotational lines of CO and H₂O. Many of these transitions fall within the waveband of the LWS and in this *Letter* we report on the first detection of thermally excited H₂O emission from an HH flow, as well as observations of lines of CO and OH.

2. Observations

LWS-grating scans (43–196.7 μm , $R = 140 - 330$), were obtained towards HH 54B ($\alpha = 12^{\text{h}}52^{\text{m}}10^{\text{s}}.6$, $\delta = -76^{\circ}40'04''$, equinox 1950.0) during ISO-revolution no. 92 on February 17, 1996. The instrument and its capabilities are described by Clegg et al. (1996) and by Swinyard et al. (1996) respectively. The ab-

* Based on observations with ISO, an ESA project with instruments funded by ESA Member States (especially the PI countries: France, Germany, the Netherlands and the United Kingdom) and with the participation of ISAS and NASA (see: Kessler et al. 1996).

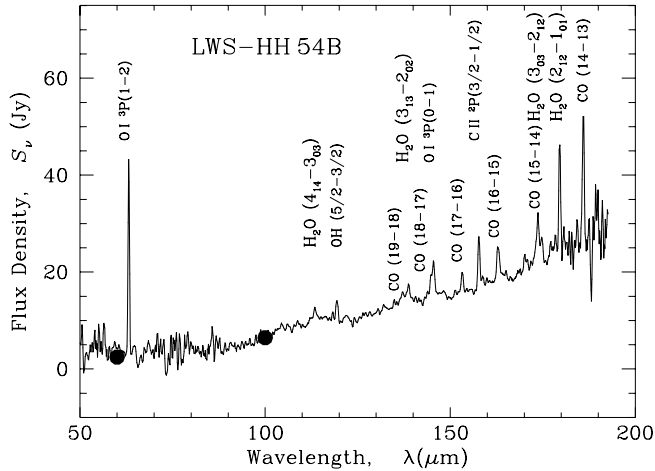


Fig. 1. LWS spectrum towards HH 54 with emission lines identified. The oversampled data have been rebinned and smoothed with a running mean filter to $\Delta\lambda = 0.42 \mu\text{m}$. The filled dots refer to IRAS data (PSC 2 + LRP + zodiacal background)

solute flux calibration is based on observations of the planet Uranus (Swinyard et al.). Full grating scans were also obtained towards HH 52, HH 53 and the CO outflow, which was mapped (3×3 , $100''$ grid). These observations are described by Nisini et al. (1996).

3. Results

The FIR spectrum towards HH 54 consists of emission lines and continuous radiation (Fig. 1). The line spectrum of HH 54 is dominated by [O I] $63 \mu\text{m}$, as expected for shocked gas. The [O I] $63/145 \mu\text{m}$ emission is intrinsic to HH 54 and compatible with the predictions of existing J-shock models, whereas the observed spatial distribution and intensity of the [C II] $158 \mu\text{m}$ line is characteristic of a PDR at the cloud surface (see: Nisini et al.).

In addition, several, weaker lines are present longward of $\sim 100 \mu\text{m}$, coinciding in wavelength with rotational transitions of CO, H₂O and OH. No such emission could be discerned in any of the other spectra of this region. All the line measurements are given by Nisini et al..

The continuum level is consistent with the sum of the zodiacal and galactic backgrounds and the dark cloud emission determined by IRAS. Situated within HH 54 is the IRAS point source 12522–7640, which has significant flux density only at $60 \mu\text{m}$ ($0.59 \pm 0.09 \text{ Jy}$). This flux can probably be ascribed entirely to [O I] line emission, for which we find (corresponding to the IRAS band) $S_{60} = 0.50 \pm 0.03 \text{ Jy}$, i.e. any stellar source would be extremely faint at these wavelengths. We conclude, therefore, that the observed diffuse radiation field is weak, a circumstance that largely simplifies the analysis of the molecular line emission in the following sections.

4. Discussion

4.1. The CO spectrum

CO emission lines from HH 54 were traced from the rotational upper level $J = 14$ to $J \lesssim 19$. The observed decrease in CO line flux with J (Fig. 1) implies that the CO emitting gas is not very highly excited and, consequently, that the emission feature at $113.5 \mu\text{m}$ is unlikely to be attributable to CO (23–22).

The quite limited spatial ($\sim 80''$) and spectral ($\sim 1500 \text{ km s}^{-1}$) resolution of the observations justified initially only average values of the physical parameters being estimated. The observed CO line ratios are reasonably well fit by a model of HH 54, where the average kinetic temperature of the gas is $T_{\text{kin}} = (330 \pm 30) \text{ K}$ and the logarithmic volume density (in cm^{-3}) is $\log n(\text{H}_2) = 5.3 \pm 0.2$ (Fig. 2). The hydrogen column density of the model, $N(\text{H}_2) = 5.0 \cdot 10^{20} \text{ cm}^{-2}$, is larger by three orders of magnitude than that of the hot H₂ gas. We assume that the relative abundance of carbon monoxide molecules $X(\text{CO}) = [N(\text{CO})/N(\text{H}_2)] = 8 \cdot 10^{-5}$.

Further, the absolute flux level of the observed CO lines then implies that only about $f_b = (10 \pm 2)^{-1}$ of the LWS-beam is filled by the emission. Hence, we derive the CO source size $\sim 25''$ to $30''$ (0.03 pc), comparable to the extent of HH 54 at optical and NIR wavelengths.

The excitation and radiative transfer calculations were all performed in the Sobolev approximation using a Large Velocity Gradient code. The Einstein A values and energies were adopted from Chackerian & Tipping (1983), with collisional excitation rate coefficients, extrapolated beyond $J = 20$ to $J = 25$, being taken from Schinke et al. (1985). An intrinsic line width of 10 km s^{-1} was adopted, a choice which will be justified below (sect. 4.3), and all CO transitions were found to be optically thin. Our model of the CO emission is not particularly sensitive to the choice of line widths, as long as $\Delta v > 0.5 \text{ km s}^{-1}$.

The total cooling rate in the CO lines from HH 54 is found to be $L_{\text{CO}} = 1.0 \cdot 10^{-2} L_{\odot}$. The thickness of the emitting layer is $dr = N(\text{H}_2)/n(\text{H}_2) = 2.5 \cdot 10^{15} \text{ cm}$ and, hence, the mass of the molecular material is $6.8 \cdot 10^{-3} M_{\odot}$.

For the lower rotational transitions, the predictions of our model can be compared to observations obtained from the ground. Towards HH 54, spectra of CO(1–0) and (2–1) have been obtained with the 15 m SEST (L. Knee, private communication). At 5.0 km s^{-1} from line centre, the intensities are $T_{\text{mb}}(1-0) = (0.36 \pm 0.06) \text{ K}$ and $T_{\text{mb}}(2-1) = (0.71 \pm 0.08) \text{ K}$. The corresponding values of our model would be somewhat less than 0.075 K and 0.82 K for the (1–0) and (2–1) transitions respectively. It thus appears that the observed lowest transition is dominated by the cold component ($\sim 15 \text{ K}$) of the extended outflow, whereas the warm gas contributes significantly to the (2–1) line. This assertion could be further tested by (2–1) mapping and SEST observations in the (3–2) line for which the predicted on-source radiation temperature is 5.7 K .

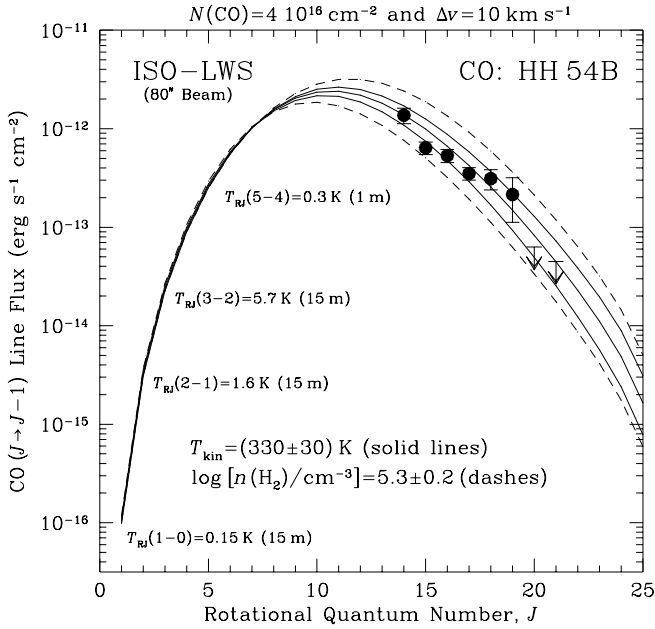


Fig. 2. Observed CO line fluxes towards HH 54 as function of the rotational quantum number of the upper state are compared to model calculations described in the text. Shown errors are statistical and are 1σ for unblended lines and 2σ for blends and upper limits. The predicted radiation temperatures of the lower transitions for 15 m and 1 m telescopes are also indicated

4.2. The H₂O and OH spectra

Keeping all parameters of the CO model of HH 54 fixed, we computed the ortho- and para-water spectra with the H₂O abundance, $X(\text{H}_2\text{O})$, as the only free parameter. For both, the number of included energy levels was 45, involving 164 transitions, several of which are masing. The radiative transition rates are those of Chandra et al. (1984), whereas for the collision rates we used the H₂O–He values ($\times 1.35$) presented by Green et al. (1993). The distribution of the ortho and para forms was assumed to be in the ratio of the statistical weights of their nuclear spins (3 : 1). As for the CO computations, the radiation field included both the cosmic microwave background and that of the diffuse dust emission (Sect. 3), the effects of which on the level populations are relatively minor, though.

The data are well represented by the adopted CO model and a water abundance $X(\text{H}_2\text{O}) = 10^{-5}$, i.e. $[\text{H}_2\text{O}/\text{CO}] \sim 10^{-1}$. Similarly, this model fits the OH spectrum as well, for $X(\text{OH}) = 10^{-6}$ (44 transitions from the HITRAN database, Rothman et al. 1987, with collision rate coefficients from Offer et al. 1994). In Fig. 3, the modeled intensities of CO, OH and H₂O, convolved with the instrumental profile, are shown superposed onto the observed spectral line data. The water spectrum is very sensitive to changes of the model parameters: the fact that the 179.5 μm line, connecting to the ground state of ortho-H₂O, is observed to be the strongest, puts severe constraints on both the temperature and density of the emitting gas. The overall success of the model, viz. the capability to simultaneously fit the CO, OH and

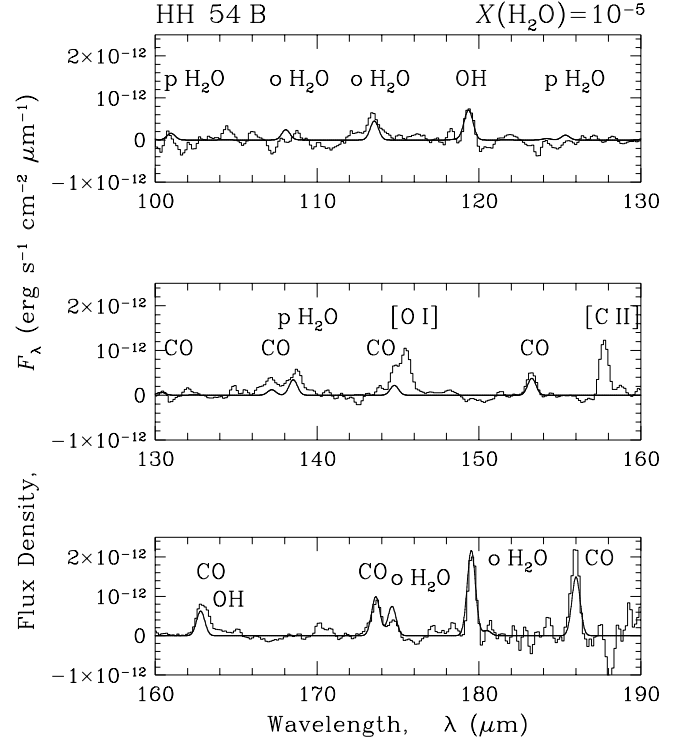


Fig. 3. The computed H₂O, OH and CO spectra, convolved with the LWS instrumental profile for $R(\lambda)$, are shown by the continuous line, superposed onto the LWS observations of HH 54, displayed in histogram form. The abundances for the fit are $X(\text{OH}) = 10^{-6}$ and $X(\text{H}_2\text{O}) = 10^{-5}$

H₂O observations, lends credence to the probable uniqueness of our model of HH 54.

The H₂O lines identified in Fig. 3 originate from levels within $E/k \sim 300$ K above ground and, with the exception of the 138.5 μm para-line, are all optically thick ($\tau \gtrsim 1$ to ~ 70). The opacity in the 557 GHz ortho ground state transition is $\tau \sim 60$ and we predict a line temperature of about 0.3 K for future observations with the 1 m-dish aboard the Odin satellite. The total rotational line cooling, due to both ortho- and para-H₂O, amounts to $L_{\text{H}_2\text{O}} = 2.0 \cdot 10^{-3} L_{\odot}$, i.e. about 20% of that due to CO, being ten times more abundant. The OH cooling rate is half of that of H₂O. Hence, the radiative losses from HH 54 through CO, OH and H₂O line emission are $\sim 1.3 \cdot 10^{-2} L_{\odot}$. Anticipating the results of the next section, the mechanical power input is $L_k = \frac{1}{2} \mu m_{\text{H}} n_0 v_s^3 \times \text{area} = 1.8 \cdot 10^{-2} L_{\odot}$, so that more than 70% is radiated away in the CO, OH and H₂O lines. In view of the uncertainties involved it is not excluded that essentially all (with some dust cooling) of the shock luminosity is radiated by these species alone.

4.3. Excitation of the molecules

In the absence of a strong radiation field the most likely physical mechanism of excitation of HH 54 is collisional heating by shock waves. The relatively low temperatures derived above

(~ 300 K) are indicative of rather slow shocks, whose velocities are of order 10 km s^{-1} . The compression of the gas behind the shocks is given by $n_{\text{max}}/n_0 = C v_s/p$, where $C = 77$ for v_s in 100 km s^{-1} , and where $p = B_{0\perp}/n_0^q$ relates the normal component of the pre-shock magnetic field, $B_{0\perp}$, to the pre-shock density, n_0 (see: Hollenbach et al. 1989). Crutcher et al. (1993) found $B_{0\perp} < 16 \mu\text{G}$ for dark clouds (average density $n(\text{H}) \sim 2 \cdot 10^3 \text{ cm}^{-3}$) so that $p \lesssim 0.4$ for $q = 0.5$. Taking n_{max} to be the observed post-shock value of the volume density, i.e. $2 \cdot 10^5 \text{ cm}^{-3}$, and using $v_s = 10 \text{ km s}^{-1}$ leads to $n_0(\text{H}_2) \lesssim 10^4 \text{ cm}^{-3}$. The value of p is uncertain by at least a factor of two, affecting the estimate of the pre-shock density accordingly.

Kaufman & Neufeld (1996) have recently presented detailed model calculations of molecular, non-dissociative C-shocks. The lowest pre-shock density (10^4 cm^{-3}) considered in these models is of the order of our estimate for the conditions in HH 54. Low-velocity models for $\log n(\text{H}_2) = 4.0$ reproduce our CO, OH and H₂O observations very well, with the observed line ratios falling in between the models for $v_s = 10 \text{ km s}^{-1}$ and 15 km s^{-1} respectively. On the basis of the previously estimated source solid angle, viz. $\Omega_{\text{source}} = 1.8 \cdot 10^{-8} \text{ sr}$ (Sect. 4.1), the lower shock velocity of 10 km s^{-1} would be favoured by the model's absolute fluxes. In this case, model fluxes would be in very good agreement with the observations, i.e. within the observational error of the brighter lines, the exception being the OH 119 μm doublet which would appear underestimated by the model by a factor of two to three.

Although the identification of C-shocks as the exciting agent of the molecules seems basically correct in the case of HH 54, a few comments may be in order. (1) The C-shock models have been computed for planar, stationary shock waves. However, our estimates of the shock parameters are close to those where C-shocks may become unstable, developing cooler clumps of neutral material (Wardle 1990). The clumpy morphology of HH 54 would be qualitatively in accord with such a scenario. In addition, the brightness variability of the H₂ (1, 0) S(1) line reported by Gredel (1994) is a clear indicator of non-stationary flows: the time scale of this variability $\lesssim 10$ yr, significantly shorter than the flow time scale, which is estimated to be $\sim 10^2$ yr. (2) The models assume that $p = 1.0$, implying *uncompressed* field strengths of at least $141 \mu\text{G}$. This certainly appears excessive for *dark clouds* by large factors. The effect of a significantly reduced value of p would be to *increase* the post-shock temperature (Hollenbach et al. 1989). When comparing with observations, this could mean that one is using the incorrect diagnostics. (3) Emission from higher excitation material, e.g. in the NIR, is outside the domain of C-shock excitation. A unifying shock model would thus be desirable. E.g., models of wide bow shocks have yet to be developed to the level of sophistication as those of Kaufman & Neufeld. Needless to say that further progress on the observational side would require improved spatial and spectral resolution.

5. Conclusions

In short, we conclude the following:

1. The shocked flow HH 54 has been successfully observed with the LWS. The spectrum of thermally excited H₂O lines is the first obtained towards an HH-object.
2. The high- J CO transitions present in the spectrum are used to estimate the physical characteristics of the line emitting regions. This CO model fits simultaneously also the observed OH and H₂O spectra for abundances $X(\text{OH}) = 10^{-6}$ and $X(\text{H}_2\text{O}) = 10^{-5}$ respectively.
3. Essentially all of the weak-shock energy of HH 54 is dissipated in rotational lines of CO, OH and H₂O.

Acknowledgements. RL enjoyed interesting discussions with M. Kaufman and D. Neufeld and we thank them for making available to us the results of their C-shock models. We thank P. Bergman for the LVG code and appreciate the valuable suggestions made by the referee, E. van Dishoeck.

References

- Chackerian C.Jr., Tipping R.H., 1983, J.Mol.Spec. 99, 431
 Chandra S., Varshalovich D.A., Kegel W.H., 1984, A&AS 55, 51
 Clegg P.E. et al., 1996, this volume
 Crutcher R.M., Troland T.H., Goodman A.A., Heiles C., Kazès I., Myers P.C., 1993, ApJ 407, 175
 Graham J.A., Hartigan P., 1988, AJ 95, 1197
 Gredel R., 1994, A&A 292, 580
 Green S., Maluendes S., McLean A.D., 1993, ApJS 85, 181
 Hollenbach D.J., Chernoff D.F., McKee C.F., 1989, in: Proc. 22nd Eslab Symp. on Infrared Spectroscopy in Astronomy, ESA SP-290, p. 245
 Kaufman M.J., Neufeld D.A., 1996 ApJ 456, 611
 Kessler M. et al., 1996, this volume
 Knee L.B.G., 1992, A&A 259, 283
 Nisini B. et al., 1996, this volume
 Offer A.R., van Hemert M.C., van Dishoeck E.F., 1994, J. Chem. Phys. 100, 362
 Rothman L.S. et al., 1987, Appl. Opt. 26, 4078
 Schinke R., Engel V., Buck U., Meyer H., Diercksen G.H.F., 1985, ApJ 299, 939
 Schwartz R.D., Dopita M.A., 1980, ApJ 236, 543
 Swinyard B.M. et al., 1996, this volume
 Wardle M., 1990, MNRAS 246, 98